



## EFFECT OF TURBULENCE ON DEFLAGRATION TO DETONATION TRANSITION

D.D. Radford, C.K. Chan and R.S. Azad<sup>†</sup>

AECL, Whiteshell Laboratories, Pinawa, Manitoba, Canada R0E 1L0

<sup>†</sup>Department of Mechanical Engineering, University of Manitoba, Winnipeg, Manitoba, Canada R3T 2N2

### ABSTRACT

*The interaction of a turbulent jet and an expanding flame kernel was examined using spark-schlieren photography and piezo-electric pressure transducers. Experiments were performed in a 9 by 9 cm, 4-m-long shock channel. Results show that an expanding flame kernel can be locally, or partially, quenched by flame stretching. The mixing of the hot combustion products, containing reactive species, with the unburnt gas in the turbulent flame-jet, created pockets of sensitized mixture. The subsequent re-ignition of the sensitized mixture could result in a local explosion. In a number of experiments the blast waves produced in the local explosion developed into detonation waves. A local explosion occurred only if there was partial quenching of the flame kernel. Partial quenching occurs when the Karlovitz-Kovaszney factor approaches unity and, therefore, it is possible to establish a set of conditions in terms of turbulent parameters for the transition to detonation.*

### 1. INTRODUCTION

In CANDU<sup>TM</sup> reactors, during some postulated loss of coolant accidents (LOCA) with also the loss of emergency cooling (LOEC), hydrogen gas can be produced by a metal-steam reaction. Under certain circumstances, the hydrogen can leak into the containment building and form a combustible mixture. The magnitude of the pressure wave resulting from the burning of the combustible mixture, and hence the damage potential, depends directly upon whether the mode of combustion is a deflagration or a detonation. Direct initiation of detonation in such a scenario is very unlikely because it would require a high-energy ignition source, which is not present in a reactor. However, if the appropriate conditions were present, a detonation could occur through a deflagration to detonation transition. A detonation wave could result in large dynamic pressure loadings on structures, or essential equipment and, therefore, a fundamental understanding of the transition process is required to properly assess the potential consequences of such accidents.

Qualitatively, the effect of turbulence on deflagration to detonation transition is well understood. In a review paper by Lee and Moen [1], it was conclusively demonstrated that turbulence plays a central role in all aspects of transition; not only in the formation of the critical conditions leading up to a local explosion, but also in the creation of the necessary environment for the amplification of the blast wave to a detonation wave. They also outlined the classical view on the role of turbulence in deflagration to detonation transition. That is, turbulence enhanced burning, or the positive aspects of turbulence, cause transition. Currently, it is not possible to predict *a priori* whether transition can occur for a given set of conditions because a quantitative theory of transition does not exist. Consequently, there have been many investigations [1-9] involving deflagration to detonation transition in turbulent reactive flows. These studies have provided insight into many aspects of flame propagation within vortex structures, entrainment and flame quenching caused by turbulence. A number of these investigations, however, contradict the classical view on the role of turbulence and suggest that flame quenching, or the negative aspects of turbulence, ultimately cause transition.

Investigations involving jet-ignition experiments [6-8] indicated that turbulent mixing of hot combustion products with unburnt gases could cause transition to detonation in the absence of turbulence-induced flame acceleration. In all of these experiments, a propagating flame was vented into a container of combustible gas, thus forming a turbulent flame-jet. The formation of the turbulent flame-jet and subsequent ignition of the gas was examined using streak and schlieren photography and piezo-electric pressure transducers. Transition to detonation occurred as a result of hot combustion products being entrained into the vortex structure of the turbulent flame-jet. The hot combustion products were mixed within the flame-jet and a subsequent localized

explosion lead to transition. Ungut and Shuff [8] developed a criterion for transition in a flame-jet based on a minimum energy release rate and the characteristic time scales of chemical kinetics and fluid dynamics. This criterion demonstrated that for successful transition to detonation, a minimum amount of hot combustion products had to be mixed with unburnt gas to result in explosive combustion and a fast rate of energy release.

A number of experiments involving flame-vortex interactions further demonstrated the role of flame quenching and entrainment in deflagration to detonation transition. Cattolica and Vosen [3] used two-dimensional laser-induced fluorescence imaging to provide a visual distribution of the OH concentration within a burning vortex-ring structure. This work quantitatively demonstrated the mechanism of flame quenching resulting from shear at the interface of the vortex and the mechanism of reactive species entrainment into the vortex core.

In a similar experiment, Jarosinski et al. [4] examined the interaction of a vortex-ring with a laminar flame and observed that ignition of the vortex occurred due to the entrainment and mixing of hot combustion products in the vortex core. When a certain amount of hot combustion products were mixed with cold unburnt gas in the vortex core, ignition would occur. They concluded that local quenching caused by flame stretching at the flame-vortex interface may play an important role in determining the subsequent burning rate of the gas.

Chan et al. [5] investigated deflagration to detonation transition resulting from burning in a confined two-dimensional vortex. They also observed that the high-velocity gradients within the confined vortex could locally, or partially, quench an expanding flame kernel. It was postulated that the mixing of the hot combustion products with the unburnt gas sensitized the gas mixture within the vortex. After an incubation time, a local explosion could occur in the sensitized mixture. In some instances, the blast waves associated with the local explosion were amplified via the SWACER mechanism [9] and deflagration to detonation transition occurred.

A common feature in the above independent studies is that transition to detonation is due to a local explosion within the core of a vortex structure. The results suggest that a minimum amount of hot combustion products have to be entrained into the vortex core in order to achieve a sufficient rate of energy release to cause transition. The hot combustion products will contain reactive species that are formed as the flame is locally quenched and entrained into the core. The presence of reactive species and non-uniform temperature distributions were shown [10,11] to greatly enhance transition to detonation in combustible mixtures. This suggests that flame quenching, or the negative aspects of turbulence, play an important role in deflagration to detonation transition.

The objective of the present investigation is to further examine the role of turbulence in deflagration to detonation transition. To accomplish this, a series of experiments was conducted to study the interaction of a transient turbulent H<sub>2</sub>-O<sub>2</sub> jet and an expanding flame kernel. By controlling the size of the expanding flame kernel before it interacted with the turbulent jet, the effect of flame quenching on deflagration to detonation transition was examined, using spark-schlieren photography and piezo-electric pressure transducers.

## 2. EXPERIMENTAL PROCEDURE

Experiments were performed in a 9 by 9 cm, 4-m-long shock channel, as shown in Figure 1. The channel consisted of a high-pressure (driver) section that was filled with helium and a low-pressure (test) section that was filled with a stoichiometric H<sub>2</sub>-O<sub>2</sub> mixture at an initial pressure (P<sub>0</sub>) of 20 kPa. Four piezo-electric pressure transducers (PCB-model 105b12) were mounted along the top of the test section and were used to monitor the events of the experiments. The test section also was equipped with 25.4-mm-thick, tempered glass windows allowing direct photographic observation of the experiment.

To initiate an experiment, an incident shock wave was formed by evacuating the driver section of the shock channel and back-filling it with helium to a pressure of approximately 370 kPa. A mylar burst disk separating the test section and the driver section was then punctured using a pneumatic plunger, forming an incident shock wave (M<sub>s</sub> = 1.9). The incident shock wave propagated into the test section of the shock channel and collided with the block-pipe arrangement, as shown in Figure 2. Part of the incident shock wave propagated down the pipe located in the centre of the block and exited at the outlet end of the pipe creating a three-dimensional turbulent jet. Before the incident shock wave arrived at the block-pipe arrangement, the combustible H<sub>2</sub>-O<sub>2</sub> gas mixture was ignited by discharging a 0.05-μF capacitor, charged to 30 kV across the cross-wire arrangement of the trigger plate, as shown in Figure 2. This created an expanding flame kernel at the outlet end of the block-pipe arrangement. The time between the ignition of the mixture at the outlet end of the block-pipe arrangement and the arrival of the incident shock wave was defined as the ignition lead time (τ<sub>lead</sub>). The size of the flame

kernel was controlled by the ignition lead time, where a longer ignition lead time resulted in a larger flame kernel.

The velocity of the incident shock wave was determined from calculations based on the pressure-time histories, as recorded on pressure transducers  $P_1$  and  $P_2$ . The events of a number of experiments were also monitored using a single-pass, spark-schlieren photographic arrangement. The spark light source was generated by discharging a 0.05- $\mu$ F capacitor, charged to 20 kV, across a 1-cm air gap. The duration of the light pulse was approximately 1.5  $\mu$ s, which was short enough to provide a clear image of the flame structure.

It was photographically observed that the expanding flame kernel diameter ( $d_{kernel}$ ) ranged from approximately 2 to 40 mm for ignition lead times in the range of 0 to 400  $\mu$ s. During this time, the flame speed of the expanding flame kernel ( $v_{kernel}$ ) was approximately constant at a flame speed of 50 m/s, which agreed well with published data [12]. Therefore, the growth rate of the flame kernel diameter as a function of ignition lead time was determined to be approximately 0.1 mm/ $\mu$ s.

On the basis of results from a previous investigation [5], it was postulated that the amount of flame quenching that took place in the turbulent flame-jet was inversely proportional to the size of the flame kernel prior to the interaction. Therefore, the amount of quenching that occurred in the turbulent flame-jet was controlled by the ignition lead time. A total of ninety six experiments were performed in which ignition lead times ranged from approximately -100 to 400  $\mu$ s. The strength of the incident shock was selected to minimize the possibility of auto-ignition of the gas mixture when it collided with the block-pipe arrangement.

### 3. RESULTS AND DISCUSSION

#### 3.1 Reaction Zone Velocity

One of the measurements used to characterize the outcome of the interaction of the flame kernel and the turbulent jet was the average velocity of the reaction zone ( $v_{reac}$ ). It was calculated by,

$$v_{reac} = \frac{\Delta x_{34}}{\Delta t_{34}} \quad (1)$$

where,  $\Delta x_{34}$  was the distance between  $P_3$  and  $P_4$ , and  $\Delta t_{34}$  was the time it took for the flame to travel between  $P_3$  and  $P_4$ . Photographic observations showed that the spacing between the flame front and the associated pressure wave was approximately constant as they travelled between pressure transducers  $P_3$  and  $P_4$ . Therefore, the flame velocity  $v_{reac}$  was interpreted to be equal to the average pressure wave velocity between  $P_3$  and  $P_4$ . Figure 3 shows  $v_{reac}$  as a function of  $\tau_{lead}$  for all of the experiments. From Figure 3 it appears that in the region where  $\tau_{lead}$  ranged from 100 to 400  $\mu$ s,  $v_{reac}$  was approximately 1000 m/s. This value corresponds closely to the choked deflagration velocities ( $v_{reac} \approx 1000$  m/s) for such mixtures and indicates that the reaction zone essentially propagated as a deflagration front. In the region where  $\tau_{lead}$  ranged from -100 to 100  $\mu$ s the values of  $v_{reac}$  were slightly higher, ranging from 1100 to 1500 m/s. For a number of experiments higher velocities ( $v_{reac} > 2000$  m/s) occurred. These velocities are of the same order as the Chapman-Jouguet detonation velocity ( $V_{cj} \approx 2500$  m/s) for the mixture and indicated that for those experiments the burning of the turbulent flame-jet resulted in transition to detonation between pressure transducers  $P_3$  and  $P_4$ .

#### 3.2 Resultant Shock Wave Pressure

The other measurement used to characterize the outcome of each experiment was the pressure ratio ( $P^*$ ), defined as,

$$P^* = \frac{P_o + \Delta P_i + \Delta P_e}{P_o + \Delta P_i} \quad (2)$$

where,  $P_o$  is the initial pressure in the test section of the shock channel and  $\Delta P_i$  is the initial pressure rise caused by the pressure waves associated with the burning of the turbulent jet. The term  $\Delta P_e$  represents a further

increase in the pressure caused by blast waves associated with a local explosion. These terms are represented on typical pressure-time histories recorded at pressure transducer  $P_3$  and are shown in Figure 4. The pressure ratio ( $P^*$ ) represents the relative strength of the blast wave associated with a local explosion resulting from the interaction of the turbulent jet and the expanding flame kernel. The values of  $\Delta P_i$  and  $\Delta P_c$  were taken from the over-pressures measured at pressure transducer  $P_3$  for all of the experiments.

The pressure ratio  $P^*$  represents the relative strength of the blast wave associated with the local explosion and is shown as a function of  $\tau_{lead}$  in Figure 5. On the basis of these results it appears that in the region where  $\tau_{lead}$  ranged from 100 to 400  $\mu\text{s}$ ,  $P^*$  was approximately 1. This corresponds to an over-pressure of approximately 30 kPa suggesting a relatively slow, overall burning rate. In the region where  $\tau_{lead}$  ranged from -100 to 100  $\mu\text{s}$  the values of  $P^*$  were higher, ranging from approximately 2 to 10. The magnitude of  $P^*$  in this region suggests an increase in the burning rate, which caused the formation of blast waves. This increase in the burning rate also caused an increase in the reaction zone velocity, as outlined in Section 3.1. In a number of experiments higher resultant shock wave pressures were observed ( $P^* > 15$ ) and were of the same order as the Chapman-Jouguet detonation pressure ratio ( $P_{c_j}/P_o \approx 17$ ). These results agree with the reaction zone velocity results and suggest that for a number of experiments, for  $\tau_{lead}$  in the range of -100 to 100  $\mu\text{s}$ , transition to detonation occurred.

### 3.3 Photographic Examination

The reaction zone velocities and the resultant shock wave pressure results indicate that there was a difference in the burning of the turbulent flame-jet as a function of  $\tau_{lead}$ . Therefore, schlieren photographs were taken for a series of tests where the ignition lead time was long (340  $\mu\text{s}$ ) and relatively short (5  $\mu\text{s}$ ).

#### 3.3.1 Long Ignition Lead Time

The flame kernel diameter before the arrival of the incident shock wave varied in size from approximately 12 to 40 mm, when  $\tau_{lead}$  was in the range of 100 to 400  $\mu\text{s}$  respectively. For this range of ignition lead times, the average flame velocity was approximately 1000 m/s indicating that the reaction zone essentially propagated as a deflagration front. Figure 6 is a series of schlieren photographs taken approximately 40  $\mu\text{s}$  apart from different experiments where  $\tau_{lead} \approx 340 \mu\text{s}$ . Because the photographs are from separate experiments, they can only be used to qualitatively describe the formation of the turbulent jet and its interaction with the expanding flame kernel. The basic features of this interaction, however, were very reproducible. Frames 1 to 4 of Figure 6 are from experiments ex1106\_3, ex1101\_7, ex1101\_6, and ex1106\_4 respectively.

Figure 6 includes a set of schematic diagrams corresponding to the schlieren photographs to outline the major features of the interaction of the turbulent jet and the expanding flame kernel. Frame 1 shows the initial development of the turbulent jet. The incident shock wave, expanding flame kernel and front edge of the turbulent jet are clearly visible. The incident shock has propagated through the large flame kernel and has not distorted the original shape appreciably. At the time that the turbulent jet begins to form, the diameter of the flame kernel is estimated to be approximately 40 mm. Therefore, the turbulent jet is created within the flame kernel and contains mainly burnt gases. Frames 2, 3 and 4 show the development of a large turbulent reaction zone. The entire turbulent zone essentially acts as one large turbulent flame kernel with corresponding large turbulent length scales. The outline of the flame kernel is very visible in these photographs indicating that little or no quenching of the flame kernel has occurred.

#### 3.3.2 Short Ignition Lead Time

Figure 7 is a set of schlieren photographs taken approximately 40  $\mu\text{s}$  apart from separate experiments where  $\tau_{lead} \approx 5 \mu\text{s}$ . Frames 1 to 4 of Figure 7 are from experiments ex1106\_2, ex1101\_2, ex1101\_1, and ex1106\_5, respectively. A set of schematic diagrams is also included. In frame 1 the incident shock exits the end of the pipe and clearly has not quenched the expanding flame kernel. The flow behind the shock ( $v_{gas} \approx 600 \text{ m/s}$ ), however, convects the small flame kernel away from the outlet end of the block-pipe arrangement. During this time the flame kernel grows from its original size of approximately 2 mm to approximately 15 mm. Because the flame kernel is originally small, the formation of the turbulent jet takes place in the unburnt gas. Therefore, the turbulent jet contains mainly cold, unburnt gas. In subsequent stages, as shown in frame 2 and frame 3,

there does not appear to be a distinct flame zone as was seen in Figure 7. The absence of a well defined flame structure, which is shown as dark bands in schlieren photographs, indicates that the expanding flame kernel was partially quenched. Other studies involving the interaction of flames with turbulent jets and vortex structures [3,4] showed that a flame could be quenched. In these studies, the flame was partially quenched by excessive flame stretching resulting from the high-velocity gradients during the formation of the turbulent jet.

Comparing the photographic records for tests of long and short ignition lead times clearly indicates that more quenching of the turbulent flame-jet occurred when the ignition lead time was short, or the expanding flame kernel was small. These results suggest that the amount of flame quenching was roughly inversely proportional to the ignition lead time, as postulated. That is, shorter ignition lead times caused more quenching. When the ignition lead time is short, the flame kernel is small and the turbulent jet consists mainly of unburnt gas. However, in the formation of the turbulent jet, the flame kernel is mixed with the unburnt gas. The mixing of the hot combustion products of the flame kernel, containing reactive species, with the cold unburnt gas sensitized the gas mixture within the turbulent jet. The subsequent re-ignition of the sensitized regions resulted in very high local burning rates and the formation of blast waves. This was indicated by the resultant shock wave velocities and pressures and is commonly referred to as a local explosion. The strength of the blast waves associated with a local explosion depends on the rate at which energy is released.

### 3.4 Energy Release Rate

Figure 8 shows the pressure traces recorded at pressure transducers  $P_3$  and  $P_4$  from experiment ex1031\_5, where  $\tau_{\text{lead}}$  was 340  $\mu\text{s}$ . The slow increase in pressure and the low magnitude in the trace recorded at pressure transducer  $P_3$  indicates that the energy release rate in the reaction zone was relatively low. For this experiment, the reaction zone velocity was 794 m/s between pressure transducers  $P_3$  and  $P_4$ . Figure 9 shows the pressure traces from experiment ex1031\_7, where  $\tau_{\text{lead}}$  was 13  $\mu\text{s}$ . For this experiment, the rate of pressure rise and the magnitude of the pressure recorded at pressure transducer  $P_3$  indicates that the energy release rate was much greater. In this experiment the reaction zone travelled at an average velocity of 1771 m/s. This suggests that the high-burning rate of the turbulent flame kernel had caused deflagration to detonation somewhere between pressure transducer  $P_3$  and  $P_4$ . The sharp increase in pressure and its magnitude of the pressure peak in the trace recorded at pressure transducer  $P_4$  also support this observation.

Figures 10 and 11 are the schlieren photographs of experiments ex1031\_5 and ex1031\_7 respectively. Both photographs were taken approximately 110  $\mu\text{s}$  after the incident shock wave had emerged from the end of the block-pipe arrangement. The location of pressure transducer  $P_3$  is indicated in both figures. These photographs further demonstrate that the amount of flame quenching was inversely proportional to the ignition lead time. In Figure 10 the flame structure is well defined, as indicated by the sharp dark lines in the photograph; in Figure 11, there appears to be no distinct flame structure. The subsequent burning of the turbulent flame zone shown in Figure 11, however, resulted in very high local burning rates and the formation of blast waves, as indicated by the resultant shock wave velocities and pressures. These results suggest that partial quenching of the turbulent flame-jet caused an increase in the energy release rate. This contradicts the classical view on the effect of flame quenching, that quenching causes a decrease in the energy release rate.

### 3.5 Quenching of the Expanding Flame Kernel

There are two mechanisms that can cause an expanding flame kernel to be quenched. The first is the lowering of the flame temperature by gas-dynamic expansion and the second is flame stretching as a result of turbulence. It is believed that flame stretching caused by turbulence was the dominant mechanism in the present investigation.

#### 3.5.1 Quenching Resulting From Gas-Dynamic Expansion

Although the temperature of a jet can be lowered significantly by gas-dynamic expansion, it is believed that gas-dynamic effects did not play a major role in the quenching process in the present experiment. Gas-dynamic calculations showed that the temperature of the gas in the formation of the turbulent jet would decrease from approximately 480 K to 360 K as it emerged from the block-pipe arrangement. This was assuming that the formation of the turbulent jet took place in unburnt gas. Such a decrease in unburnt gas temperature would not

significantly impair flame propagation. Furthermore, an expanding flame kernel is clearly visible in frame 1 of Figure 7 and demonstrates that gas-dynamic effects did not quench the flame.

### 3.5.2 Quenching Resulting From Turbulence

It is well known that turbulence effectively increases the overall burning rate of gas mixtures by flame folding and enhancing the heat and mass transport. Previous studies on turbulent flame propagation [13,14] have shown that the overall burning rate increases as the turbulent fluctuating velocity increases, until a certain maximum value is reached. Past the maximum value, flame quenching starts to take place and an overall decrease in the burning rate will be observed. That is, past some level of turbulent intensity, flame quenching starts to occur and causes an overall decrease in the energy release rate.

Abdel-Gayed et al. [15] demonstrated that the ratio of turbulent to laminar burning velocities ( $S_T/S_L$ ) could be represented as a function of the ratio of the root mean square (r.m.s.) turbulent velocity ( $u'$ ) to the laminar-burning velocity ( $S_L$ ). This is shown schematically in Figure 12. Initially, there is an increase in the turbulent burning velocity as  $u'$  is increased. As  $u'$  is increased further, the rate of increase of the turbulent burning velocity decreases until a maximum flame velocity is achieved. This is followed by a decrease of the turbulent-burning velocity with increasing  $u'$  because flame quenching starts to take place. Further increases in  $u'$  will eventually cause complete quenching of the flame zone. The initial dependence of the turbulent burning velocity on the r.m.s. turbulent velocity, which represents the turbulent intensity, illustrates that turbulence initially enhances the burning process by increasing the flame surface area and the transport of heat and mass. This results in an increase in the overall volumetric burning rate. However, as the turbulent intensities continue to increase, and reach critical values, the overall volumetric burning rate reaches a maximum value. Beyond this point the turbulent intensities lead to partial quenching of the reaction zone. This is caused by excessive flame stretching and cooling of the reaction zone. Further increases to the turbulent intensity result in decreasing the volumetric burning rate to the point of flame extinction, or complete quenching.

### 3.6 Quenching Criteria

Jarosinski [16] showed the quenching of flame structures due to turbulence can be correlated by the Karlovitz-Kovaszney factor ( $K_f$ ),

$$K_f = \frac{u'\delta}{LS_L} \quad (3)$$

where  $\delta$  is the laminar flame thickness,  $L$  is the integral scale of the turbulence, and the other parameters are defined in Section 3.5.2. The Karlovitz-Kovaszney factor is essentially the ratio of the characteristic chemical reaction time to the characteristic fluid dynamic time, or mixing time, of the turbulent flow. The experimental values for  $K_f$  obtained by Jarosinski [16] for complete quenching ranged from 7 to 20. Following the description of flame quenching resulting from turbulence in Section 5.5, partial flame quenching occurs when the turbulent burning velocity, or overall volumetric burning rate, approaches its maximum value. Chan et al. [5] observed that local, or partial quenching, took place when  $K_f$  was approximately 1. In the present investigation,  $K_f$  is estimated to be approximately 0.8, where  $u' \approx v_{rms} \approx 600$  m/s,  $\delta \approx 0.2$  mm,  $L \approx 19$  mm, and  $S_L \approx 7.4$  m/s [12]. Although  $K_f$  was not varied systematically in the present study, a turbulent flow having a  $K_f$  value of approximately unity can be expected to cause partial quenching of the mixture. Furthermore, photographic records in the present investigation clearly indicate that for short induction lead times the turbulent flame-jet was partially quenched.

In the previous investigation [5], burning in a confined two-dimensional vortex was examined and it was shown that an expanding flame kernel could be partially quenched because of non-uniform flow within a vortex. The partial quenching and subsequent turbulent mixing of hot combustion products with unburnt gas formed a sensitized region in the vortex. After a certain induction time, a local explosion occurred in the sensitized region and blast waves were formed. The strength of the blast wave was dependent on the size of the sensitized region and the mixture sensitivity. Based on those results, it was speculated that partial quenching can cause an increase in the rate of burning and hence, the energy release rate. That is, partial quenching can cause an

increase in the rate of energy release that cannot be obtained by flame folding and enhanced heat and mass transport alone.

Results from the present investigation further demonstrate that an expanding flame kernel can be partially quenched by turbulence. It was observed that a local explosion and the formation of blast waves only occurred when the expanding flame kernel was partially quenched. On the basis of these results, it is believed that partial quenching of a turbulent flame-jet can create local sensitized regions in a gas mixture by mixing the hot combustion products with the unburnt gases. This causes an overall reduction in the instantaneous burning rate. The subsequent re-ignition of these sensitized regions, however, can result in very high volumetric burning rates capable of generating blast waves. The energy release rate is very large in comparison to that associated with turbulent flame propagation. This can be interpreted as a "time focussing effect" of turbulence on the combustion process. Partial quenching, or the negative aspects of turbulence, results in focussing the energy that is released in the combustion process into a very small period of time, as shown in Figure 13. As the turbulence level in a reactive flow is increased, turbulent enhanced burning takes place and the overall burning rate is increased. At some critical level of turbulent intensity, local, or partial, quenching of the reaction zone occurs. Re-ignition of the sensitized regions, formed by the partial quenching and turbulent mixing, cause a very high burning rate over a short period of time. This high rate of energy release, or local explosion, is capable of producing strong blast waves, which is the essential step in deflagration to detonation transition. Since partial quenching lead to the local explosion, a quenching criteria can be used as a necessary condition for deflagration to detonation transition.

## 6. SUMMARY

The interaction of a turbulent jet with an expanding flame kernel was examined using spark-schlieren photography and piezo-electric pressure transducers. Results indicate that an expanding flame kernel can be locally, or partially, quenched as a result of the turbulence induced in the formation of a turbulent jet. The mixing of hot combustion products, containing reactive species, with the cold unburnt gas can create sensitized regions within the mixture. The subsequent re-ignition of these sensitized regions results in focussing the energy released into a very short period of time, causing very high burning rates and the generation of blast waves. This is commonly referred to as a local explosion. The blast waves generated from such a local explosion can have strengths similar to those produced in constant-volume combustion. In some experiments, the blast waves developed into detonation waves.

Results from the present investigation also indicate that a local explosion can only occur if there is partial quenching in the turbulent flow field. Since a local explosion is a necessary step in the deflagration to detonation transition, it is possible to use quenching conditions as criteria for transition. Partial quenching only occurs when the ratio of the characteristic chemical reaction and fluid dynamic time scales, represented by the Karlovitz-Kovaszney factor, approaches unity. By equating these characteristic time scales, a set of critical turbulent parameters can be obtained for a given mixture. It is then possible to establish the necessary conditions for deflagration to detonation transition for a given combustible mixture, in terms of fundamental turbulent parameters such as turbulence intensities and length scales. This demonstrates that flame quenching, or the negative aspects of turbulence, play an important role in deflagration to detonation transition.

## ACKNOWLEDGEMENTS

This work was funded jointly by AECL, Ontario Hydro, Hydro Quebec and New Brunswick Power under the CANDU Owners Group WPIR 6-0434.

## REFERENCES

1. LEE, J.H.S and MOEN, I.O., "The Mechanism of Transition from Deflagration to Detonation in Vapour Cloud Explosions", Prog. Energy Combust. Sci., 6, pp. 359-389, 1980.
2. PETERS, N. and WILLIAMS, F.A., "Premixed Combustion in a Vortex", 22<sup>nd</sup> Symposium (International) on Combustion, The Combustion Institute, Pittsburgh, PA, pp. 495-503, 1989.

3. CATTOLICA, R.J. and VOSEN, S.R., "Two-Dimensional Fluorescence Imaging of a Flame-Vortex Interaction", *Combust. Sci. Tech.*, 48, pp. 77-87, 1986.
4. JAROSINSKI, J., LEE, J.H.S. and KNYSTAUTAS, R., "Interaction of a Turbulent jet and a Laminar Flame", 22<sup>nd</sup> Symposium (International) on Combustion, The Combustion Institute, Pittsburgh, PA, pp. 505-514, 1989.
5. CHAN, C.K., LAU, D. and RADFORD, D., "Initiation of Detonation Resulting from Burning in a Confined Vortex", 23<sup>rd</sup> Symposium (International) on Combustion, The Combustion Institute, Pittsburgh, PA, in press.
6. KNYSTAUTAS, R., LEE, J.H., MOEN, I. and WAGNER, H.G., "Direct Initiation of Spherical Detonation by a Hot Turbulent Gas Jet", 17<sup>th</sup> Symposium (International) on Combustion, The Combustion Institute, Pittsburgh, PA, pp. 1235-1244, 1978.
7. MOEN, I.O., BJERKETVEDT, D., ENGBRETSSEN, T., JENSSEN, A., HJERTAGER, B.H. and BAKKE, J.R., "Transition to Detonation in a Flame-Jet", *Comb. Flame*, 75, pp. 297-308, 1989.
8. UNGUT, A. and SHUFF, P.J., "Deflagration to Detonation Transition from a Venting Pipe", *Combust. Sci. Technol.*, 63, 1&3, pp. 75-87, 1989.
9. LEE, J.H., KNYSTAUTAS, R. and YOSHIKAWA, N., "Photochemical Initiation of Gaseous Detonations", *Acta Astronautica*, 5, pp. 971-982, 1978.
10. ZEL'DOVICH, YA.B., GELFAND, B.E., TSYGANOV, S.A., FROLOV, S.M. and POLENOV, A.N., "Concentration and Temperature Non-Uniformities of Combustible Mixtures as a Reason of Pressure Wave Generation", 11<sup>th</sup> Colloq. (International) on Dynamics of Explosions and Reactive Systems, p. 88, 1988.
11. DOROFEEV, S.VB., KOCHURKO, A.S. and CHAIVANOV, B.B., "Detonation Onset Conditions in Spatially Non-Uniform Combustible Mixtures", 16<sup>th</sup> Symposium on Loss Prevention and Safety Promotion in the Process Industry, v.4, pp. 1-19, 1989.
12. KOROLL, G.W. and MULPURU, S.R., "The Effect of Dilution with Steam on the Burning Velocity and Structure of Premixed Hydrogen Flames", 21<sup>st</sup> Symposium (International) on Combustion, The Combustion Institute, Pittsburgh, PA, pp. 1811-1819, 1986.
13. AL-KHISHALI, K.J., BRADLEY, D. and HALL, S.F., "Turbulent Combustion of Near-Limit Hydrogen-Air Mixtures," *Comb. and Flame*, 54, 1983.
14. CHECKEL, M.D. and TING, D.S., "Turbulent Effects on Development Turbulent Flame in as Constant Volume Combustion Chamber", SAE Technical Paper 9308667.
15. ABDEL-GAYED, R.G., BRADLEY, D. and LAU, A.K.C., "The Straining of Premixed Turbulent Flames", 22<sup>nd</sup> Symposium (International) on Combustion, The Combustion Institute, Pittsburgh, PA, pp. 731-738, 1988.
16. JAROSINSKI, J., "A Survey of Recent Studies on Flame Extinction", *Prog. Energy Combust. Sci.* 12, pp. 81-116, 1986.

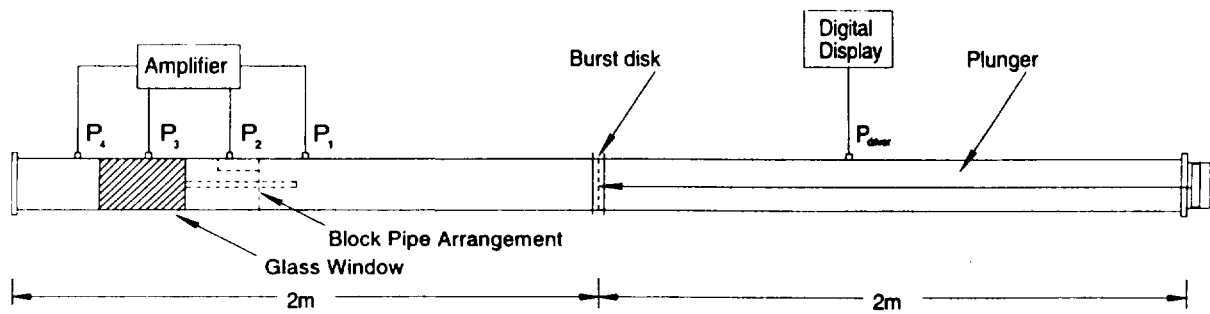


Figure 1: Schematic diagram of the shock channel and data acquisition system.

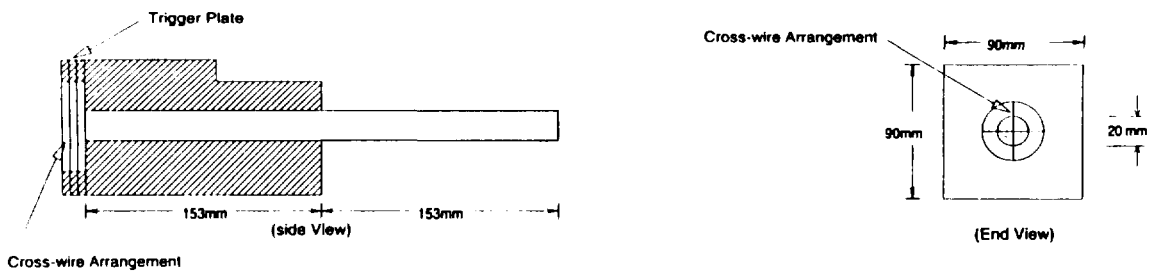


Figure 2: Schematic diagram of the block-pipe arrangement and trigger plate.

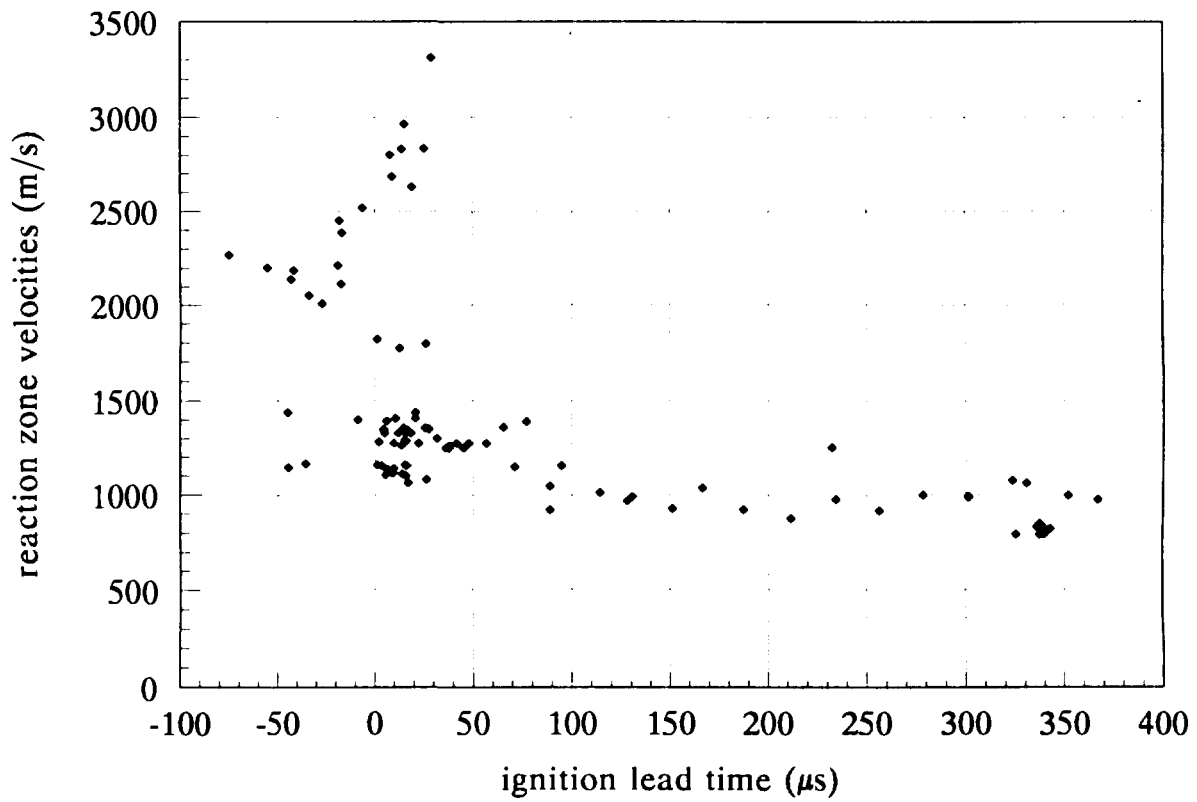


Figure 3: Reaction zone velocities as a function of the ignition lead time.

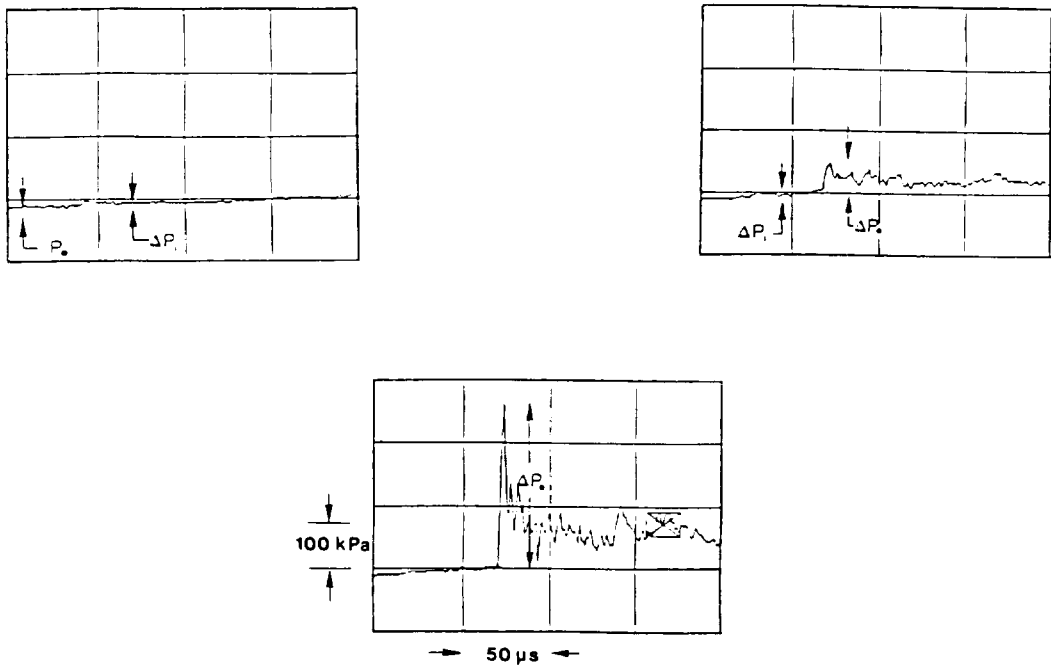


Figure 4: Typical pressure-time histories as recorded at pressure transducer  $P_3$ .

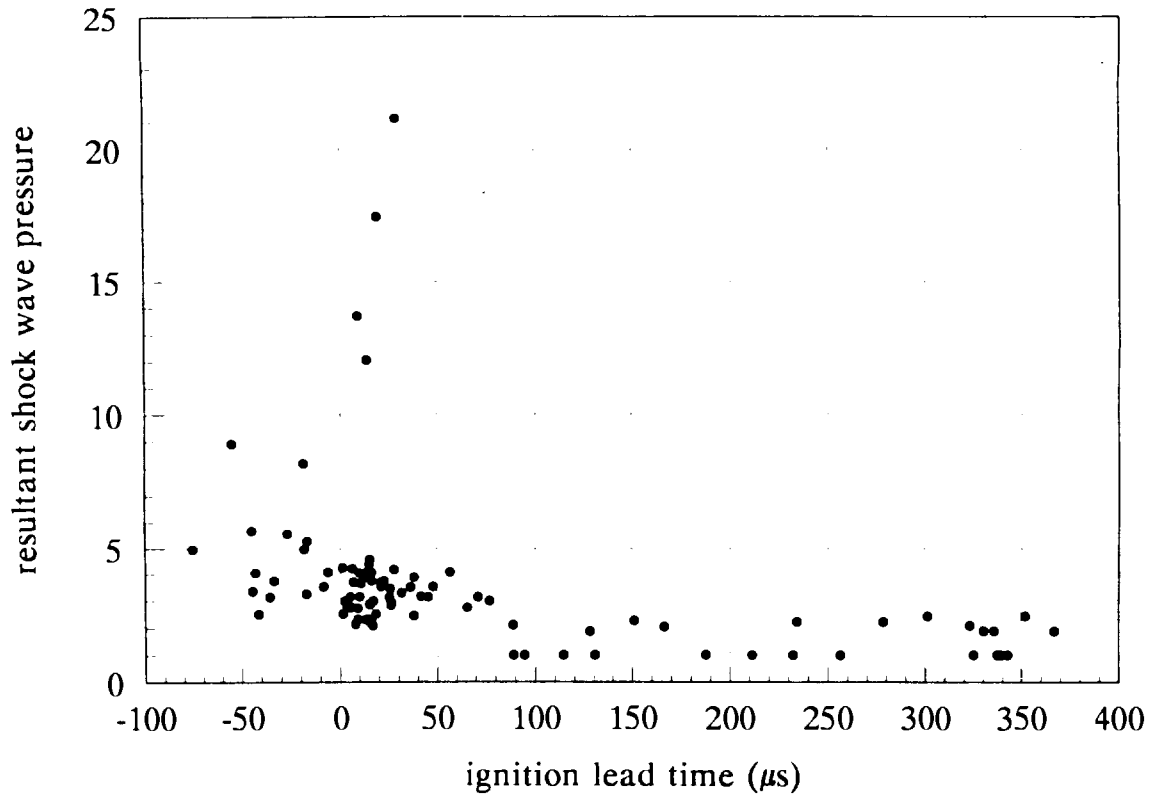


Figure 5: Resultant shock wave pressure ratio as a function of ignition lead time.

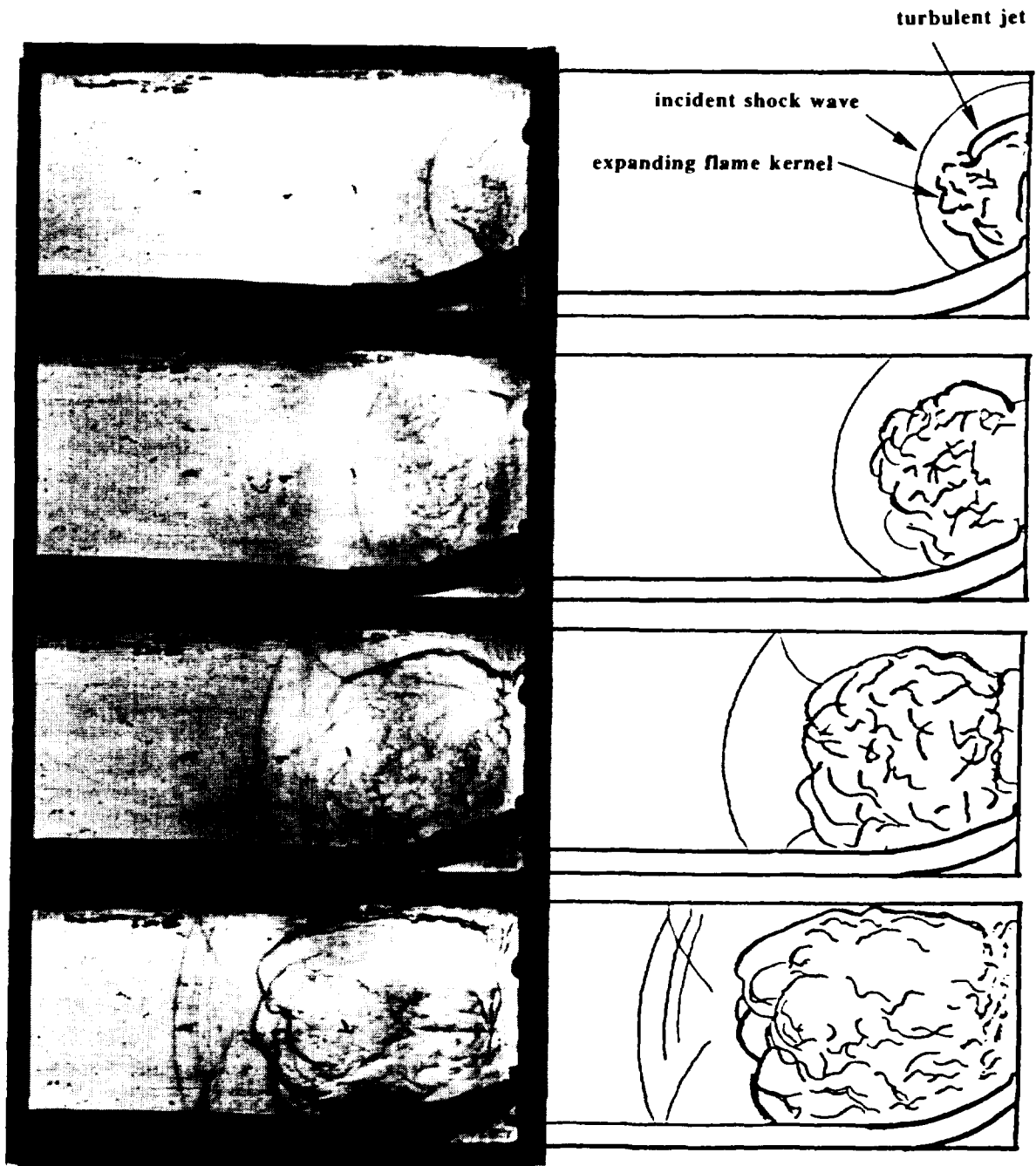


Figure 6: Schlieren photographs of the interaction of the turbulent jet and a large flame kernel. ( $\tau_{\text{lead}} = 340 \mu\text{s}$ )

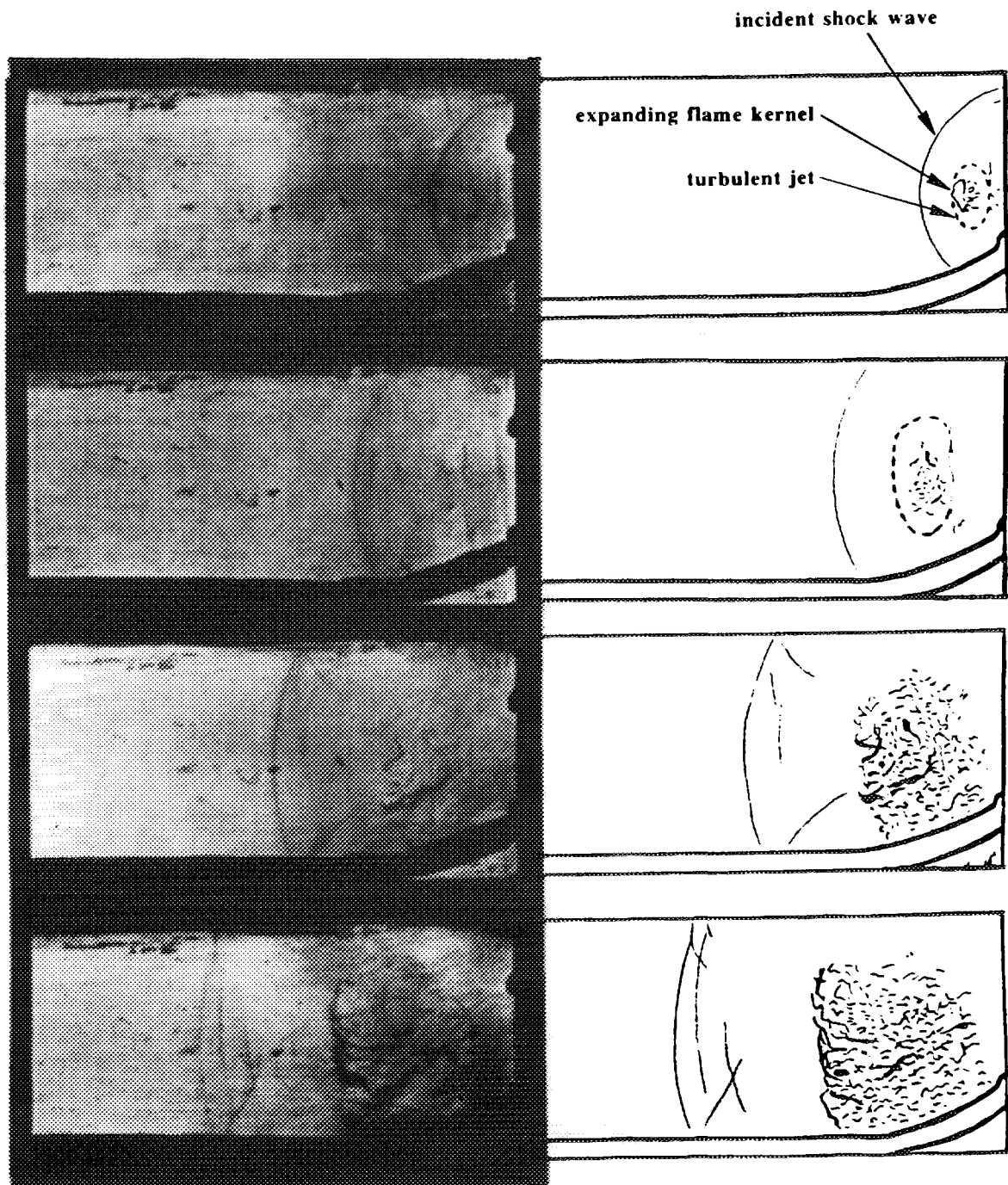


Figure 7: Schlieren photographs of the interaction of the turbulent jet and a small flame kernel. ( $\tau_{\text{lead}} = 5 \mu\text{s}$ )

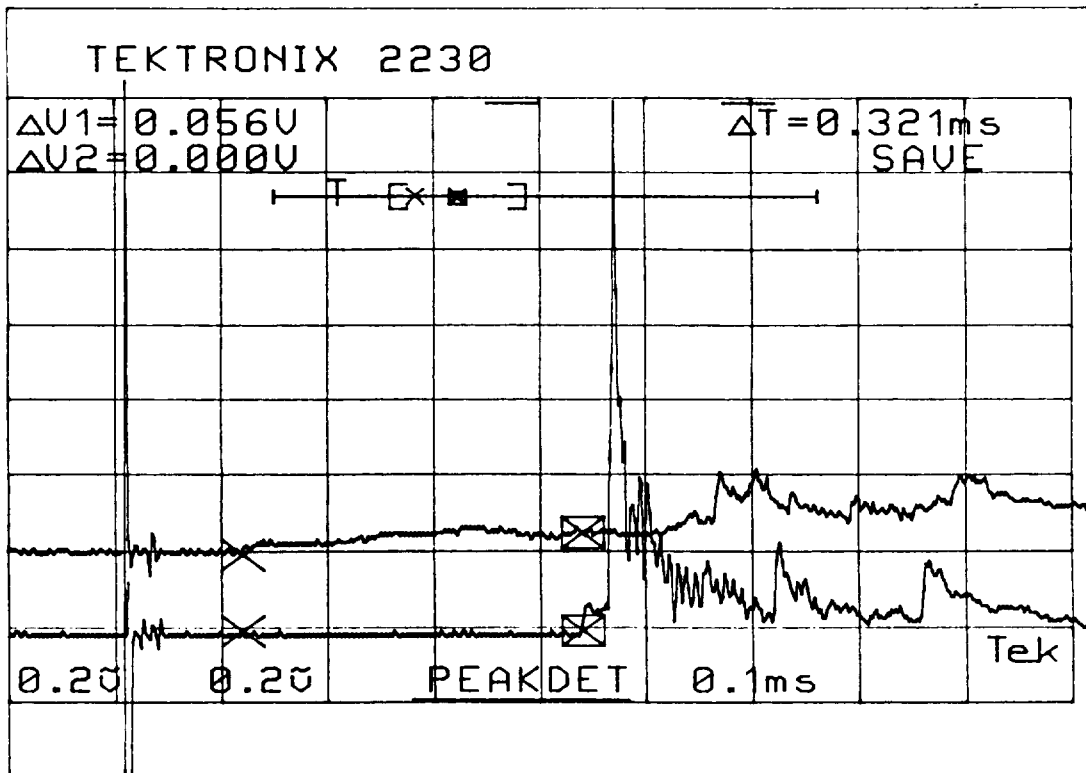


Figure 8: Pressure traces recorded at pressure transducers  $P_3$  and  $P_4$  from experiment ex1031\_5. ( $\tau_{lead} = 340 \mu s$ )

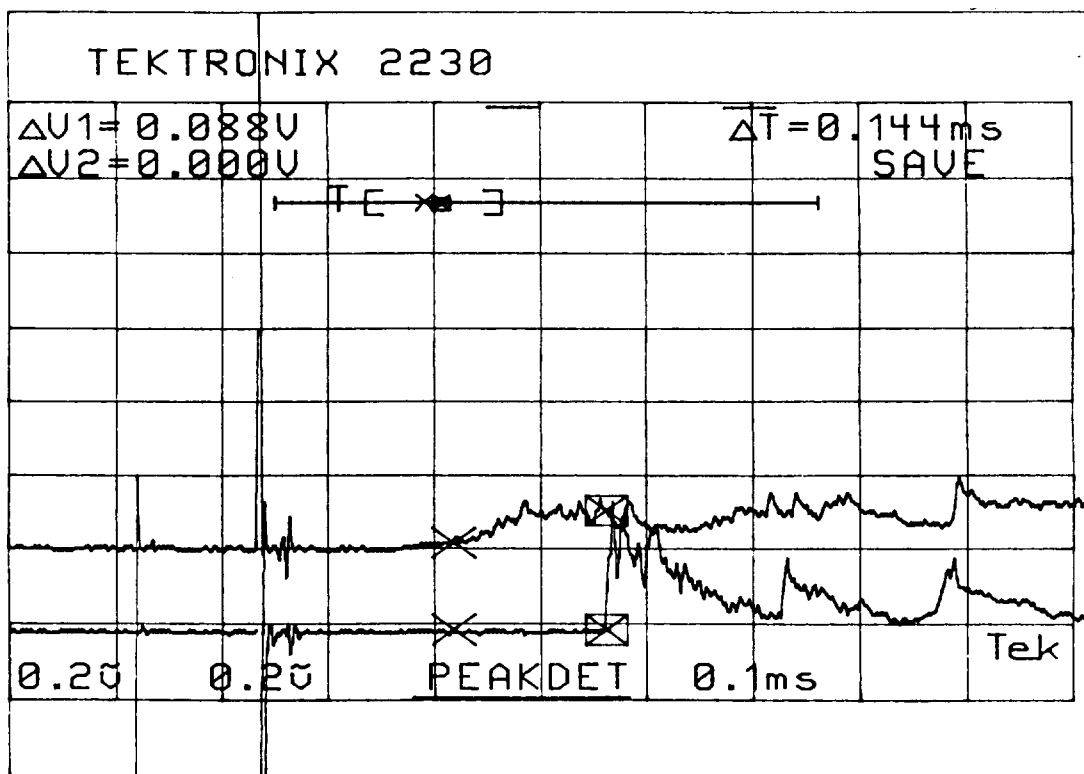


Figure 9: Pressure traces recorded at pressure transducers  $P_3$  and  $P_4$  from experiment ex1031\_7. ( $\tau_{lead} = 13 \mu s$ )



Figure 10: Schlieren photograph of turbulent flame-jet from experiment ex1031\_5. ( $\tau_{\text{lead}} = 340 \mu\text{s}$ )



Figure 11: Schlieren photograph of turbulent flame-jet from experiment ex1031\_7. ( $\tau_{lead} = 13 \mu s$ )

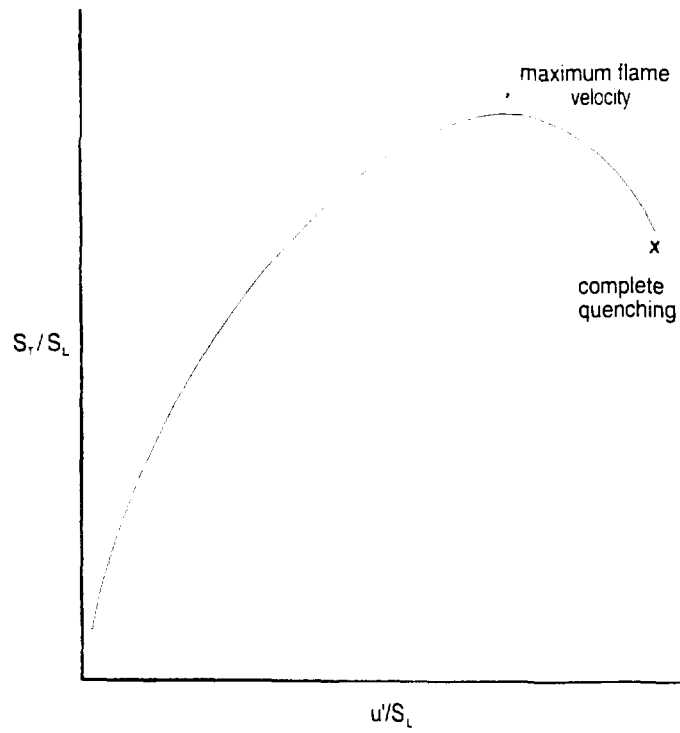


Figure 12: Effect of turbulent intensity ( $u$ ) on turbulent burning velocity ( $S_T$ ).

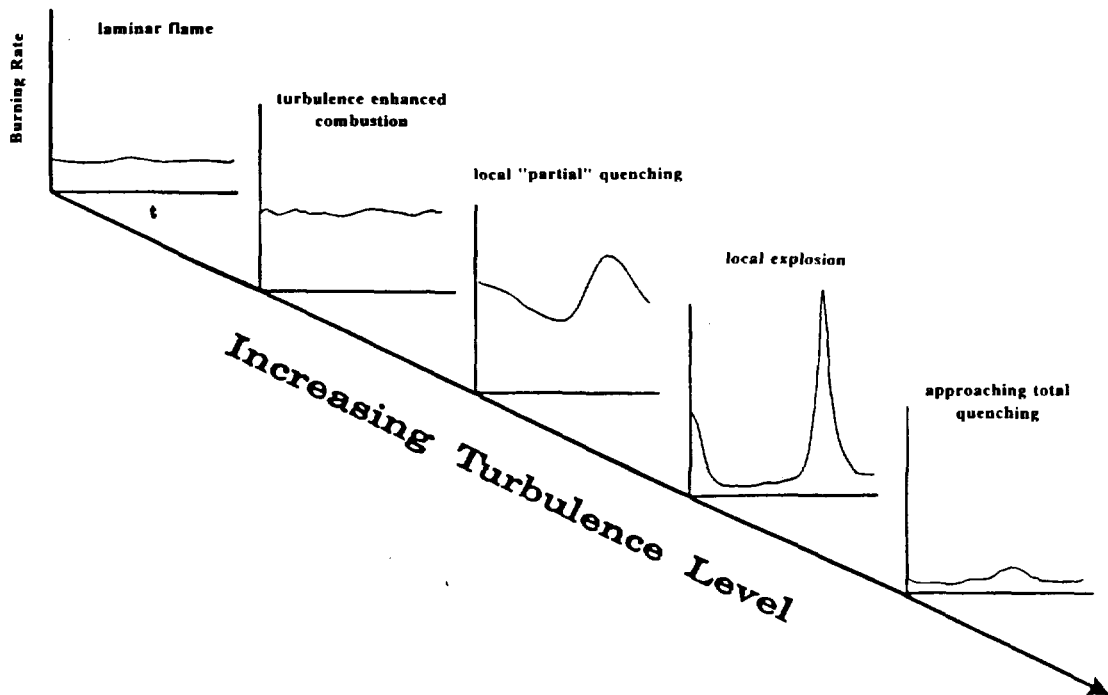


Figure 13: Effect of time focussing on energy release rate.